Science

AAAS

Interface and heterostructure design in polyelemental nanoparticles

Peng-Cheng Chen[1,2], Mohan Liu[1], Jingshan S. Du[1,2], Brian Meckes[2,3], Shunzhi Wang[2,3], Haixin Lin[2,3], Vinayak P. Dravid[1,2], Chris Wolverton[1], Chad A. Mirkin[1,2,3*]

[1]Department of Materials Science and Engineering,Northwestern University, Evanston, IL 60208, USA.
[2]International Institute for Nanotechnology, Northwestern University, Evanston, IL 60208, USA.
[3]Department of Chemistry, Northwestern University, Evanston, IL 60208, USA.

Publication date: 1st march 2019

M.P. Kannan
09/03/2019

Relevance to our group

- Single nanoparticle with multiple interface

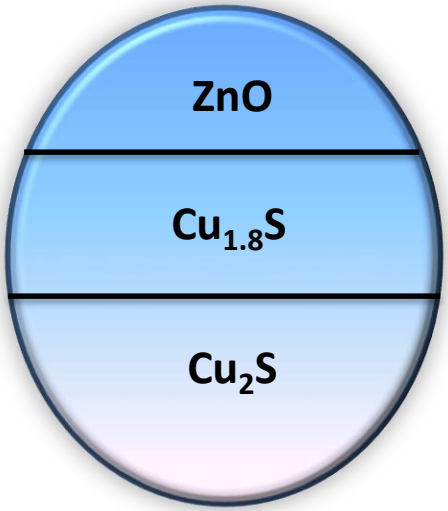

- Interface formation in High entropy alloys

Background work

Science
AAAS

Polyelemental nanoparticle libraries

Peng-Cheng Chen,[1,2] Xiaolong Liu,[3] James L. Hedrick,[2,4] Zhuang Xie,[2,5]
Shunzhi Wang,[2,5] Qing-Yuan Lin,[1,2] Mark C. Hersam,[1,3,5]
Vinayak P. Dravid,[1,2] Chad A. Mirkin[1,2,4,5*]

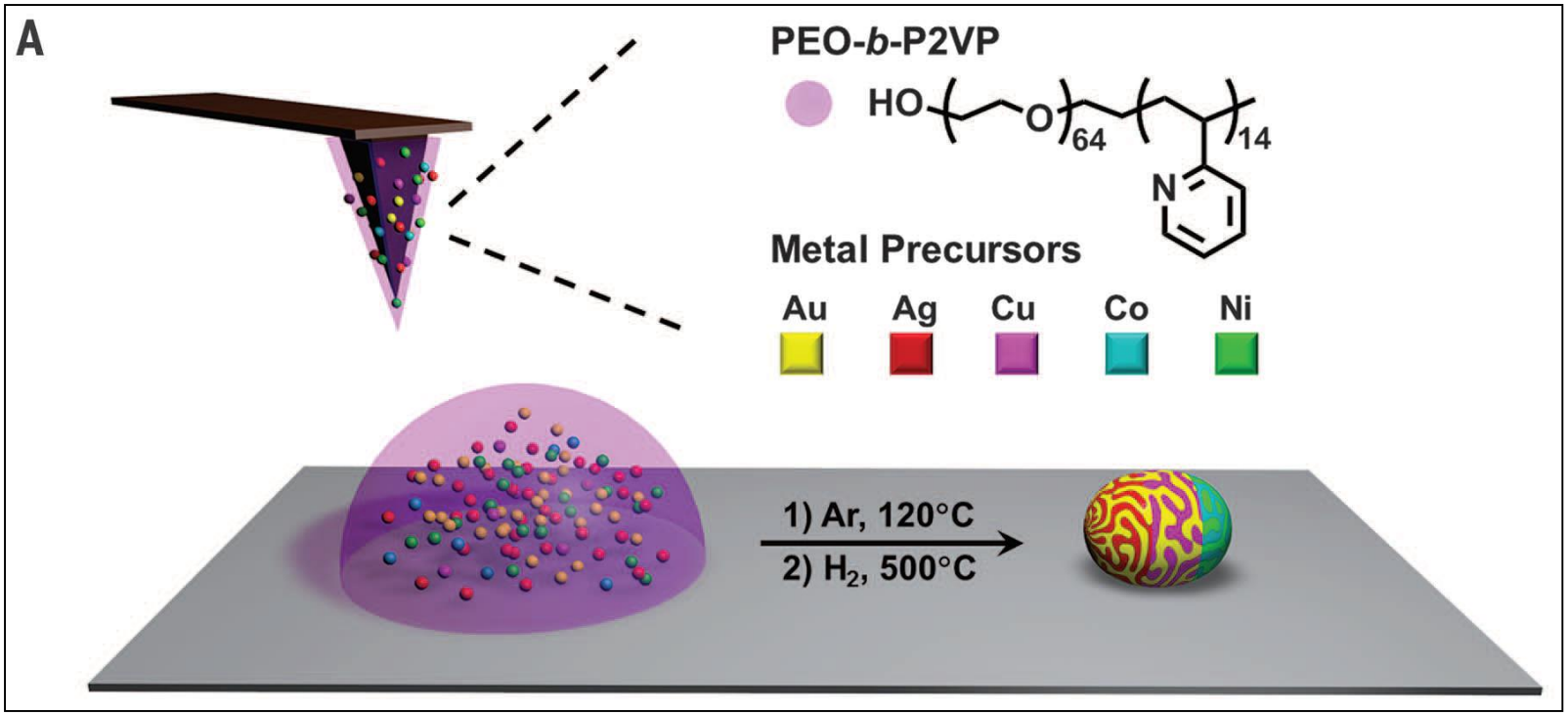

Scheme depicting the process: A polymer loaded with metal ion precursor is deposited onto a substrate in the shape of a hemispherical Dome via dip-pen nanolithography. After two-step thermal annealing, the metal precursors are aggregated and reduced, the polymer is decomposed, and individual NPs result from each dome feature. The interwoven patterns in the NP schemes are only meant to indicate the alloying of the elements and not the actual atomic structure.

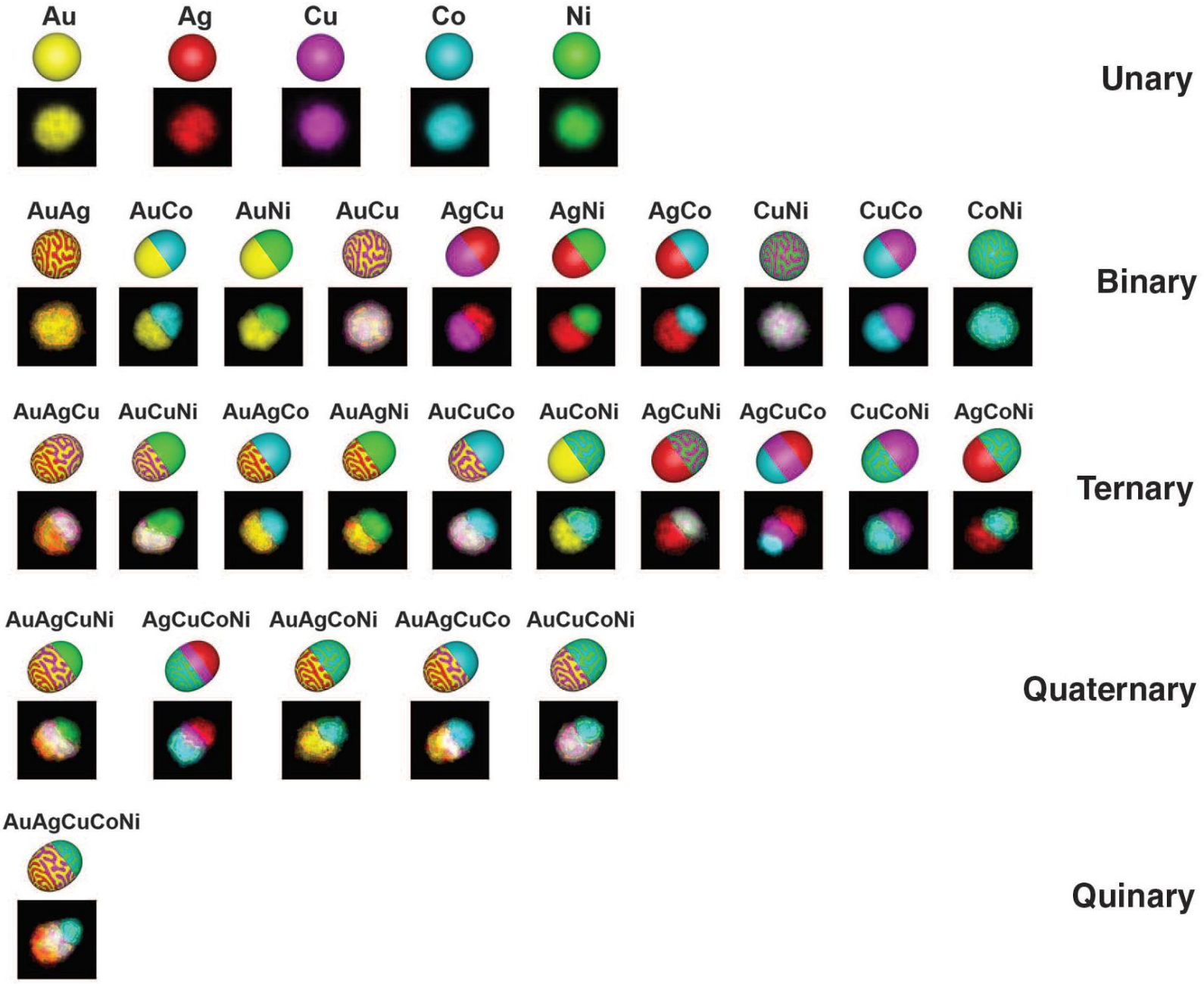
Au
Ag
Cu
Co
Ni
Unary
AuAg
AuCo
AuNi
AuCu
AgCu
AgNi
AgCo
CuNi
CuCo
CoNi
Binary
AuAgCu
AuCuNi
AuAgCo
AuAgNi
AuCuCo
AuCoNi
AgCuNi
AgCuCo
CuCoNi
AgCoNi
Ternary
AuAgCuNi
AgCuCoNi
AuAgCoNi
AuAgCuCo
AuCuCoNi
Quaternary
AuAgCuCoNi
Quinary

This paper…

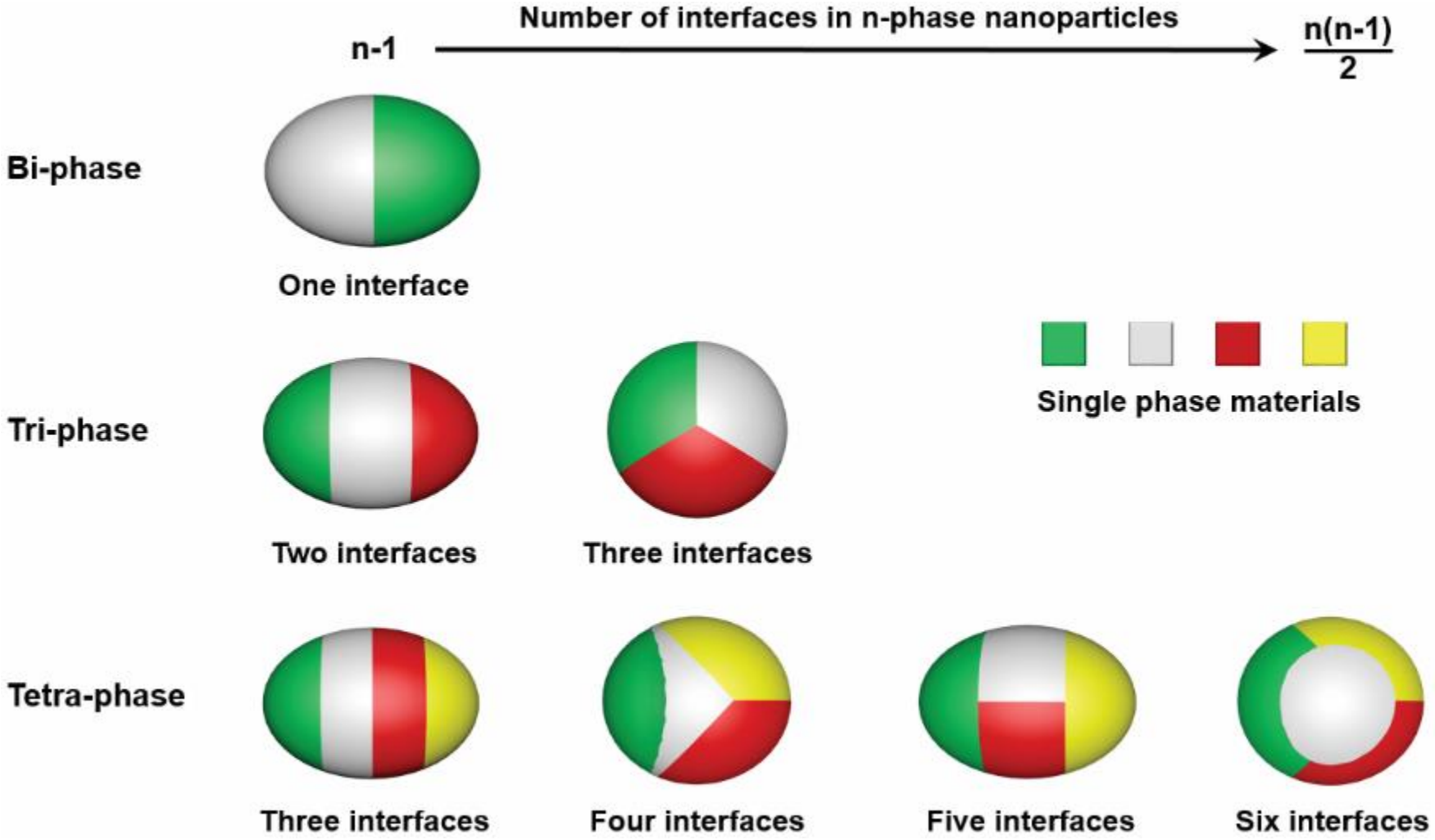

Fig. 1. Theoretically possible number of interfaces in heterodimer, heterotrimer, and Heterotetramer NPs. All of these NP architectures are observed and characterized in this work except for the tetra-phase structure with three interfaces.

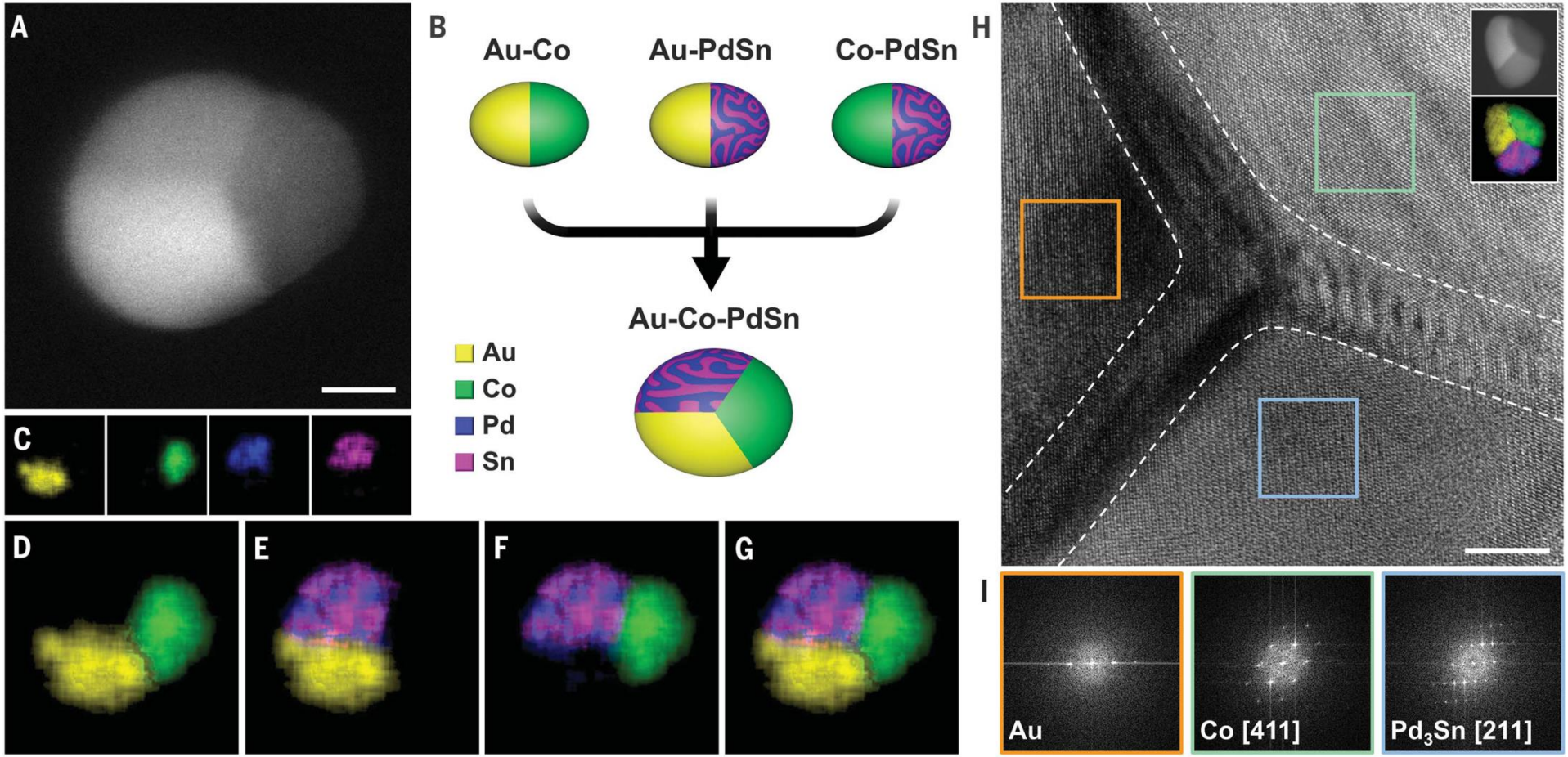

Fig. 2. Au-Co-PdSn triphase heterostructured NPs with three interconnected interfaces. (A) ADF-STEM image of a representative Au-Co-PdSn NP ($Au_{0.30}Co_{0.37}Pd_{0.19}Sn_{0.14}$). Scale bar, 10 nm. (B) Schematic illustration of the miscibility relationship among the Au, Co, and PdSn phases. (C to F) EDS elemental mapping of the NP in (A). Overlay of selected element maps shows the phase boundaries of (D) Au-Co, (E) Au-PdSn, and (F) Co-PdSn. (G) Overlay of all element maps showing the configuration of the three phases in a Au-Co-PdSn NP. (H) HRTEMimage of the triphase junction in a Au-Co-PdSn NP ($Au_{0.25}Co_{0.36}Pd_{0.29}Sn_{0.10}$). Scale bar, 3 nm. Dashed lines highlight the positions of the three phase boundaries. Insets are an ADF-STEM image and EDS mapping of the entire NP. (I) FFTs of the regions indicated in the HRTEM image.

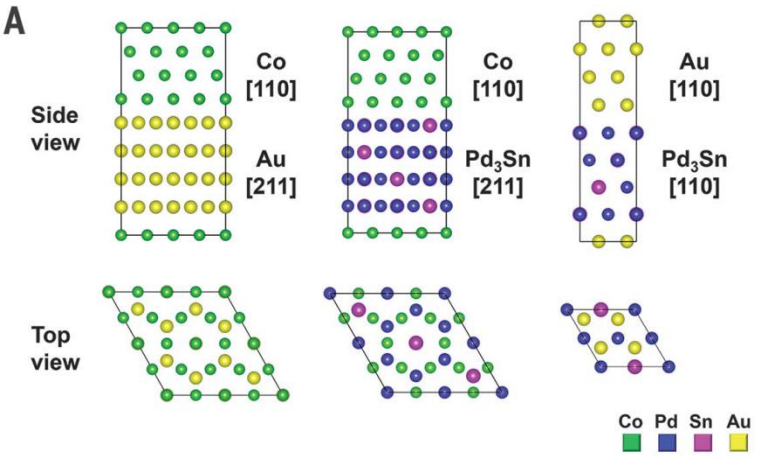

B

Interfacial energy	γ (eV/Å^2)	Surface energy	γ (eV/Å^2)
Au-Co	0.032	Au	0.046
Co-Pd_3Sn	0.048	Co	0.118
Au-Pd_3Sn	0.001	Pd_3Sn	0.083

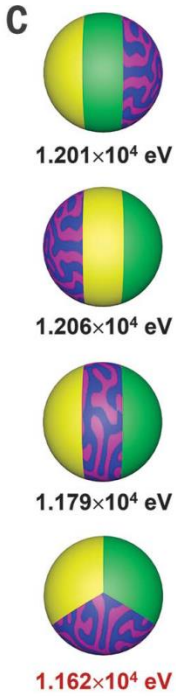

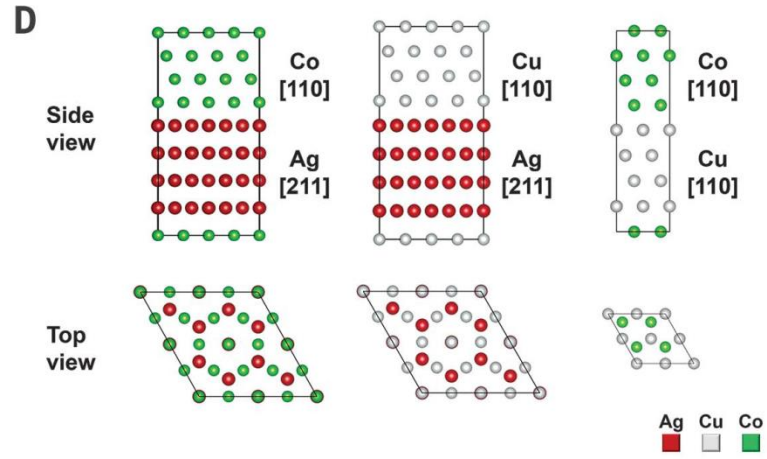

E

Interfacial energy	γ (eV/Å^2)	Surface energy	γ (eV/Å^2)
Ag-Co	0.052	Ag	0.047
Ag-Cu	0.023	Cu	0.082
Cu-Co	0.013	Co	0.118

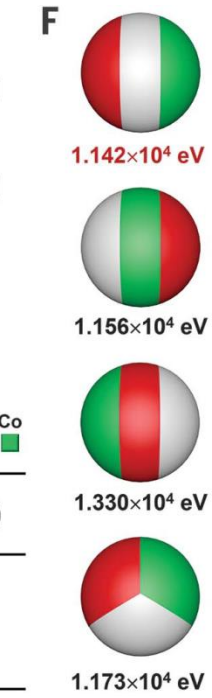

Fig. 3. DFT simulation of the architecture of Au-Co-Pd_3Sn and Ag-Cu-Co triphase NPs. (A) DFT-simulated relaxed structures of the (111) interfacial planes among Au, Co, and Pd_3Sn. (B) The surface energies of Au, Co, and Pd3Sn (111) planes and the interfacial energies among Au, Co, and Pd3Sn (111) planes. g, surface and interfacial energies. (C) Calculated total surface and interfacial energies of Au-Co-Pd_3Sn NPs with equal volumes of each phase (diameter, 20 nm). (D) DFT-simulated relaxed structures of the (111) interfacial planes among Ag, Cu, and Co. (E) The surface energies of Ag, Cu, and Co (111) planes and the interfacial energies among Ag, Cu, and Co (111) planes. (F) Calculated total surface and interfacial energies of Ag-Cu-Co NPs with equal volumes of each phase (diameter, 20 nm).

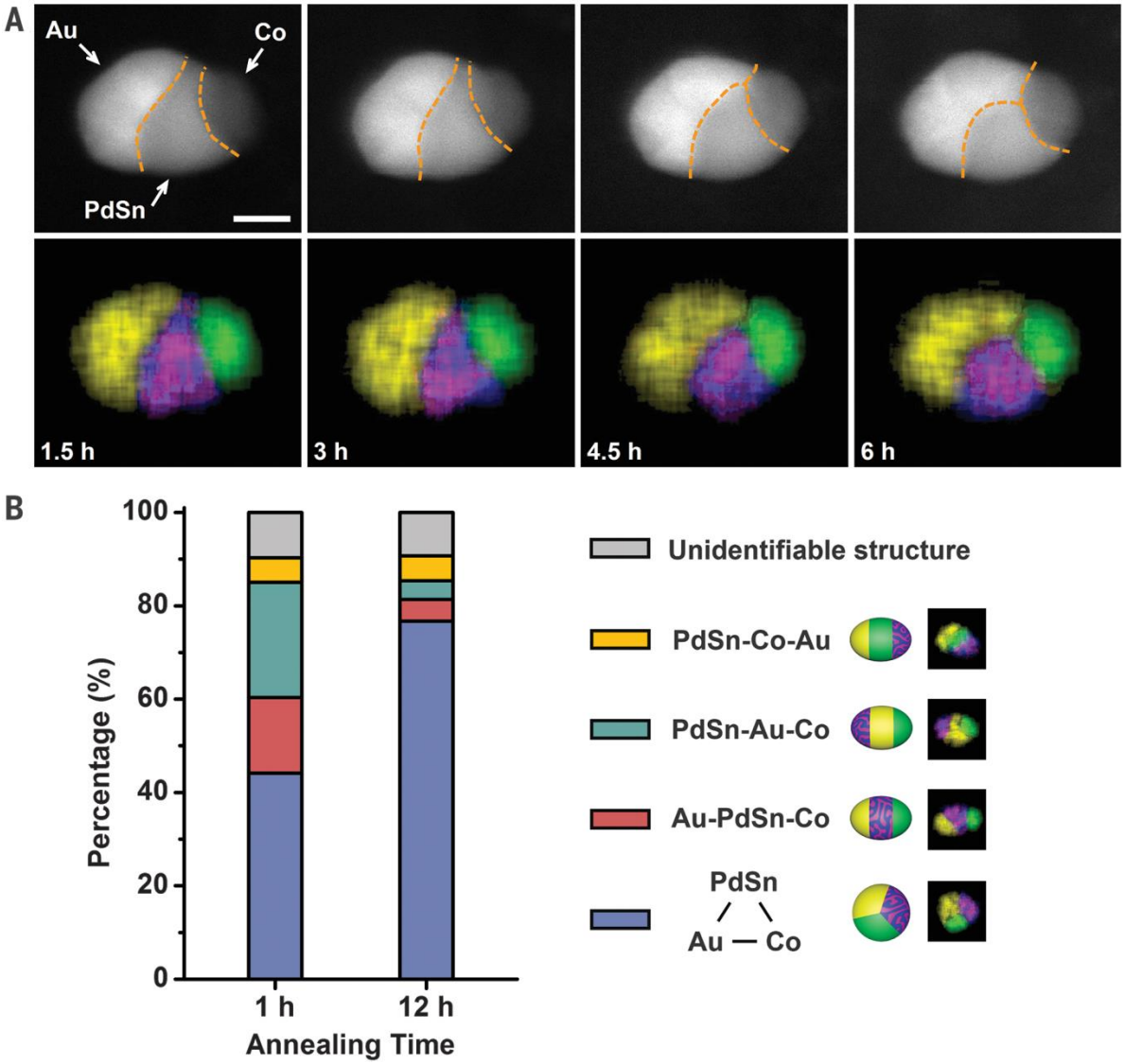

Fig. 4. Structural evolution of Au-Co-PdSn triphase NPs during thermal annealing. (A) ADF-STEM images (top row) and corresponding EDS mapping (bottom row) of a Au-Co-PdSn NP ($Au_{0.33}Co_{0.24}Pd_{0.26}Sn_{0.17}$) annealed under flowing H_2 at 500°C over time. Dashed lines Outline the positions of phase boundaries. Scale bar, 15 nm. (B) Statistical distributions of NPs (n = 150) with different architectures.

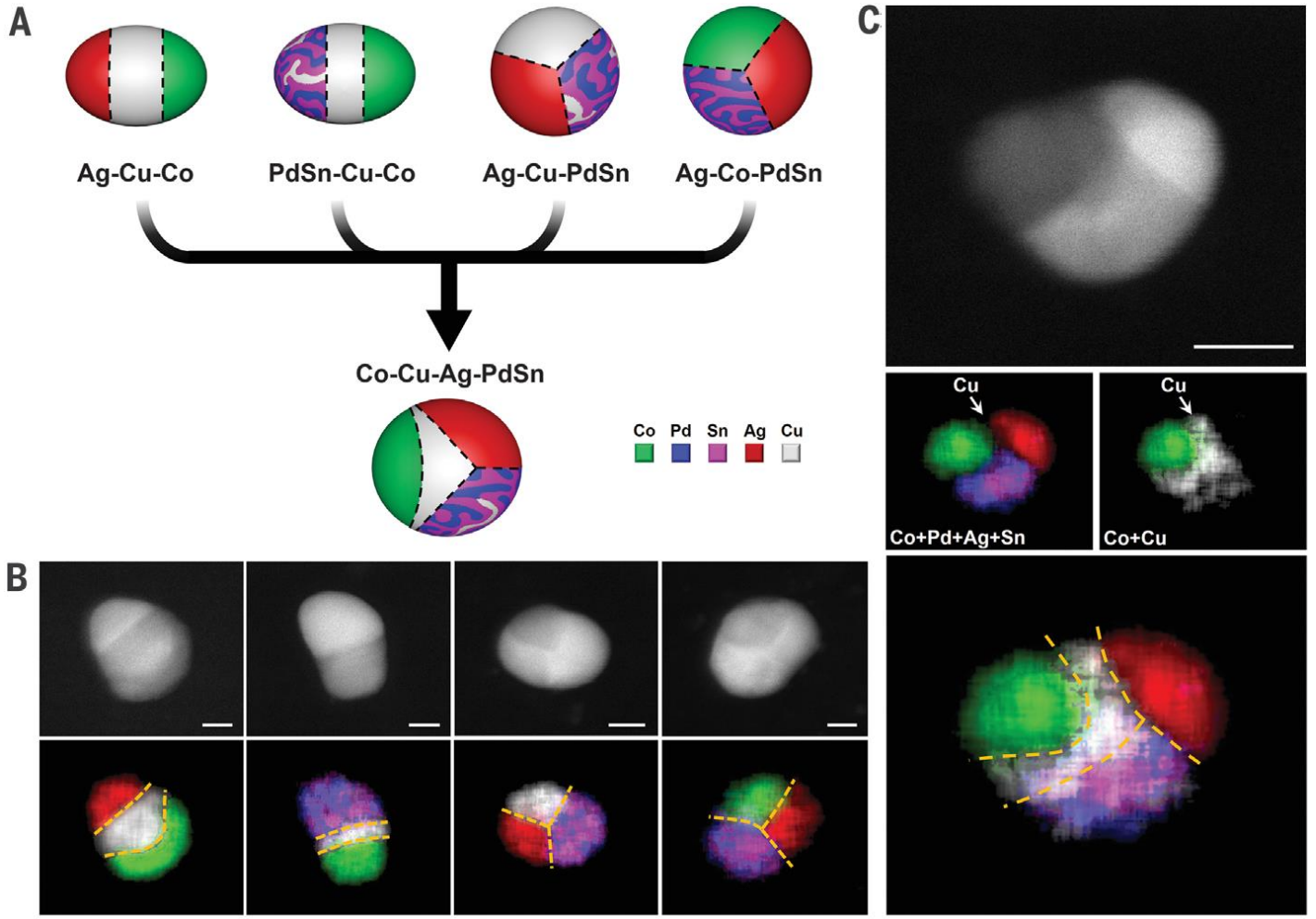

Fig. 5. Tetraphase heterostructured NPs with four and five interfaces. (A) Schematic illustration depicting the architectures of tri- and tetraphase NPs composed of Ag, Cu, Co, and PdSn phases. (B) ADF-STEM images (top row) and EDS mapping (bottom row) of representative triphase NPs for all phase combinations. The compositions of the four triphase NPs are $Ag_{0.23}Cu_{0.47}Co_{0.30}$, $Co_{0.34}Cu_{0.29}Pd_{0.21}Sn_{0.16}$, $Ag_{0.30}Cu_{0.30}Pd_{0.27}Sn_{0.13}$, and $Ag_{0.33}Co_{0.23}Pd_{0.27}Sn_{0.17}$. (C) ADF-STEM image (top row) and EDS mapping (bottom row) of a representative tetraphase NP composed of Ag, Cu, Co, and PdSn phases ($Ag_{0.32}Cu_{0.20}Co_{0.21}Pd_{0.15}Sn_{0.12}$).Overlay of selected element maps.

Scale bars, 15 nm.

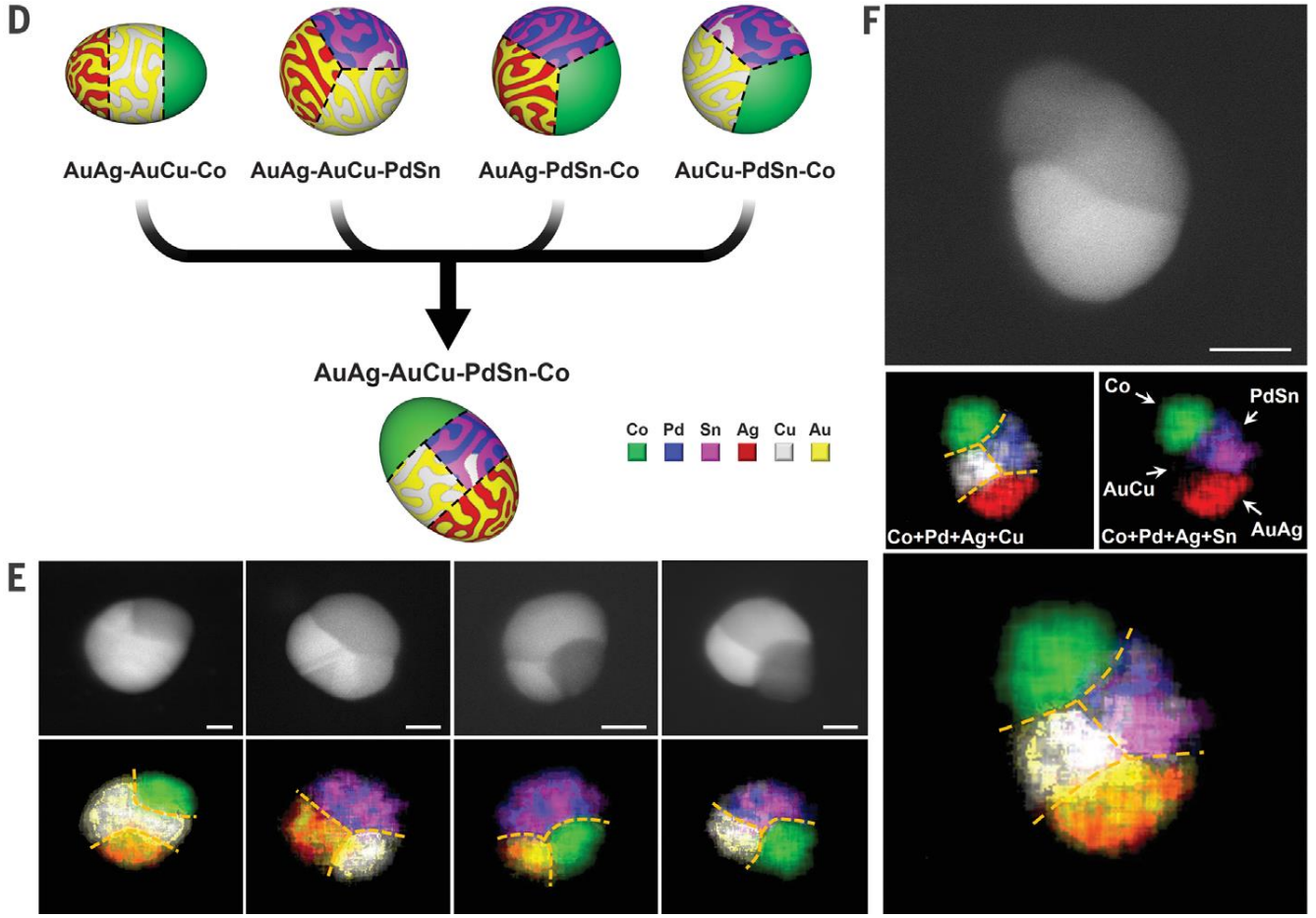

Fig. 4.(D) Schematic illustration depicting the architectures of tri- and tetraphase NPs composed of AuAg, AuCu, Co, and PdSn phases. (E) ADF-STEM images (top row) and EDS mapping (bottom row) of representative triphase NPs for all phase combinations. The compositions of the four triphase NPs are $Au_{0.30}Ag_{0.19}Cu_{0.29}Co_{0.22}$, $Au_{0.12}Ag_{0.30}Cu_{0.28}Pd_{0.20}Sn_{0.10}$, $Au_{0.06}Ag_{0.10}Co_{0.24}Pd_{0.39}Sn_{0.21}$, and $Au_{0.13}Cu_{0.27}Co_{0.30}Pd_{0.15}Sn_{0.15}$.
(F) ADF-STEM image (top row) and EDS mapping (bottom row) of a representative tetraphase NP composed of AuAg, AuCu, Co, and PdSn phases ($Au_{0.18}Ag_{0.16}Cu_{0.20}Co_{0.23}Pd_{0.13}Sn_{0.10}$). Overlay of selected element maps (middle row) shows the relative configuration of the 4 phases in NP.

Scale bars, 15 nm.

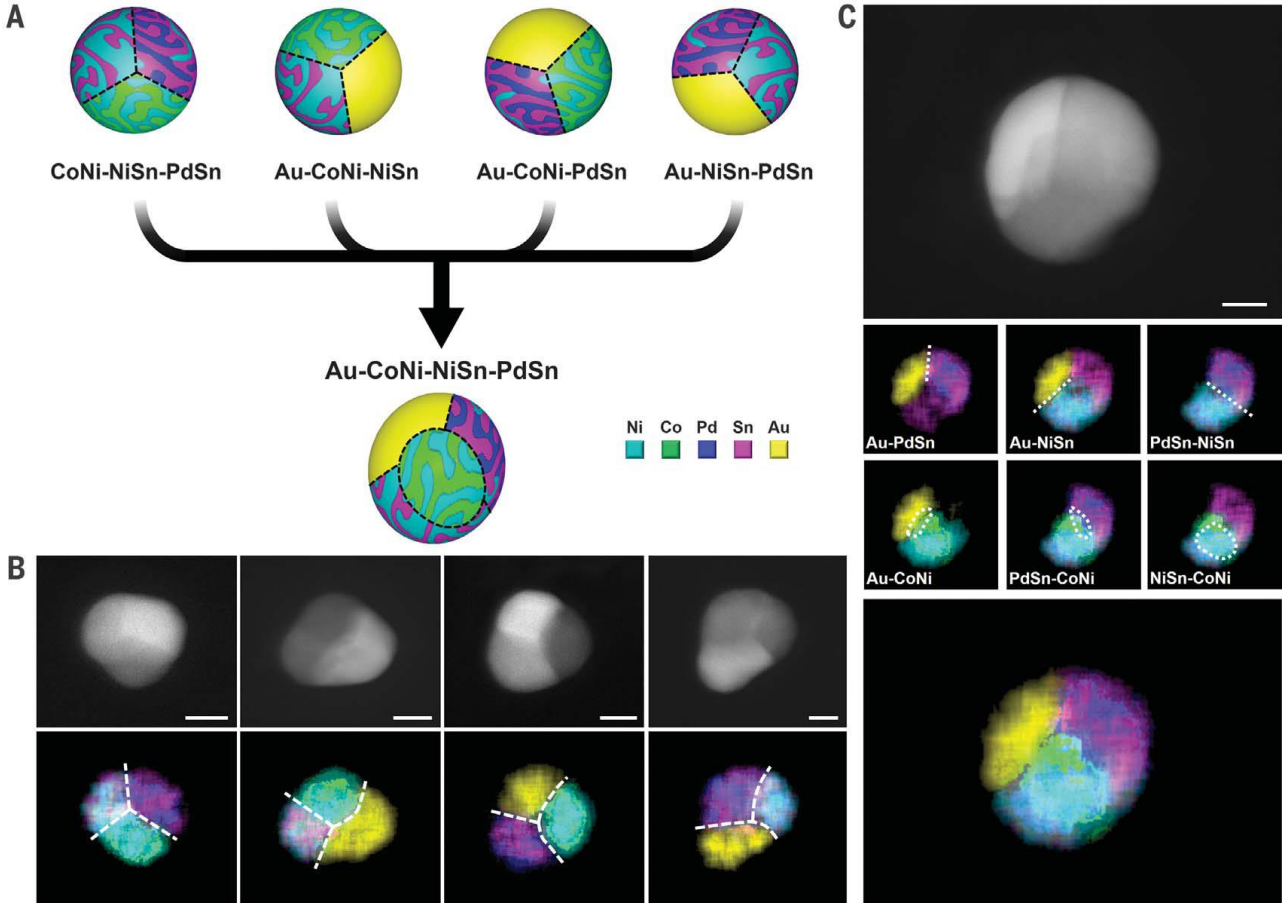

Fig. 5. Tetraphase heterostructured NPs with six interfaces. (A) Schematic illustration depicting the architectures of tri- and tetraphase NPs composed of Au, CoNi, NiSn, and PdSn phases. (B) ADF-STEM images (top row) and EDS mapping (bottom row) of representative triphase NPs for all phase combinations. The composition of the four triphase NPs are $Co_{0.13}Ni_{0.35}Pd_{0.26}Sn_{0.26}$, $Au_{0.37}Co_{0.18}Ni_{0.36}Sn_{0.09}$, $Au_{0.29}Co_{0.17}Ni_{0.19}Pd_{0.20}Sn_{0.15}$, and $Au_{0.25}Ni_{0.24}Pd_{0.20}Sn_{.3}$. (C) ADF-STEM image (top row) and EDS mapping (bottom row) of a representative tetraphase NP composed of Au, CoNi, NiSn, and PdSn phases ($Au_{0.20}Co_{0.11}Ni_{0.30}Pd_{0.21}Sn_{0.18}$). Overlay of selected elemental maps (two middle rows) shows the relative positions of any two of the four phases.

Conclusion

- A set of rules for engineering the number and types of interfaces in multiphase polyelemental NPs by using PdSn based multiphase NPs as a proof-of-concept system was presented.

- For interface engineering, the balancing of surface and interfacial energies is critical in determining the thermodynamically preferred structures for multiphase NPs, as demonstrated by the notable tetraphase polyelemental NPs described herein, with four, five, and six phase boundaries.

- Interface engineering in polyelemental nanomaterials will be essential for optimizing their use in catalysis, plasmonics, nanoelectronics, and energy harvesting.

Thank you ☺